Pressure-driven semiconductor-metal transition in intermediate-valence $TmSe_{1-x}Te_x$ and the concept of an excitonic insulator

J. Neuenschwander* and P. Wachter
Laboratorium für Festkörperphysik, Eidgenössische Technische Hochschule Zürich, CH-8093 Zürich, Switzerland
(Received 21 November 1989; revised manuscript received 9 March 1990)

This work studies the pressure-induced semiconductor-to-metal transition (SMT) in the TmSe-TmTe alloy system. This SMT is accompanied by a valence instability of the Tm ions. Single-crystalline semiconducting $TmSe_{1-x}Te_x$ alloys are investigated under high pressure at low temperatures. Measurements of electrical resistivity, magnetic susceptibility, neutron diffraction, and optical properties are presented and discussed. A very unusual peak structure in the resistivity-pressure relation is observed at low temperatures. A discussion of the novel feature involves the concept of an excitonic insulator and *f-d* hybridization. The magnetic behavior of the compounds is significantly influenced by the SMT. This is thought to be mainly due to the additional coupling between the magnetic moments of Tm via free carriers which are present in the metallic state.

I. INTRODUCTION

Among the rare-earth compounds there is a fascinating class of solids called intermediate (or homogeneously mixed) -valence compounds. The characteristic common feature of these materials is believed to be that their rare-earth constituents are not in a stable state of well-defined valence. Instead, one has a quantum-mechanical mixture of the $4f^n5d^0$ and $4f^{n-1}5d^1$ configurations on *each* rare-earth ion (also at $T=0$ K). This situation is to be distinguished from *inhomogeneously* mixed valency where one encounters divalent and trivalent ions on equivalent lattice sites [e.g., Eu_3S_4, Sm_3S_4 (Ref. 1)]. Experimental evidence for the existence of only one, nonintegral, $4f$ configuration in *intermediate-valence compounds* is given by intermediate lattice constants compared to the ones corresponding to integral valence, by magnetic susceptibility at higher temperatures, which detects the state of the $4f$ shell, by a soft lattice and a negative Poisson's ratio, and by Mössbauer spectroscopy. These examples of experimental techniques have in common that they transfer only minute amounts of energy to the electronic ground state (x-ray scattering is elastic and the Mössbauer effect transfers about 10^{-7} eV). It is generally accepted that the nonintegral $4f$ configuration is caused by a *hybridization* of localized $4f$ and extended $5d$ states near the Fermi level E_F.[2] Treating the $4f$ states as single and independent impurities as in a Kondo impurity problem, over a narrow energy range (or order 10 meV) a large density of states (DOS) occurs at E_F.[3] However, a better approach is to consider the $4f$ states to be in a regular lattice (Kondo lattice problem, hybridization lattice model) and then invariably a double-peak DOS structure near E_F appears.[3-5] When E_F lies in one of the DOS peaks the material is metallic [examples: intermediate-valence $CePd_3$, $YbCu_2Si_2$ (Ref. 6), and heavy-fermion systems[7]]. But, in other cases, E_F lies in a tiny (of order meV) forbidden gap, making the material an insulator for $T\rightarrow 0$, but also intermediate valence [example: SmB_6 (Refs. 8 and 9)]. A pseudogap (DOS is small but nonzero) may occur as in "gold" SmS.[10] High-energy measurements like *L*-, *M*-edge or x-ray-, uv photoelectron spectroscopy transfer several eV up to thousands of eV to the hybridized ground state, the binding energy of which is only about 10 meV. Thus the hybridized state breaks up at the site of absorption of the photon and decays into integer valent contributions of $4f^n5d^0$ and $4f^{n-1}5d^1$, as manifest in the spectra, the ratio of which corresponds to the degree of valence mixing.[11] A coexistence of intermediate valency and magnetic order has been found only in Tm-based compounds; this is thought to be related to the fact that the (free) Tm ion has a magnetic ground state in both valencies (Tm^{2+}:$^2F_{7/2}$ and Tm^{3+}:$^3H_6$), whereas intermediate valence compounds based on Ce, Sm, Eu, and Yb happen to mix a magnetic and nonmagnetic (free-ion) state.

We shall concentrate now on the TmSe-TmTe alloy system. These compounds crystallize in the NaCl structure (fcc lattice) and exhibit the interesting feature of a compositionally induced *semiconductor-to-metal transition* (SMT). TmTe, on the one end of the system, is an ionic semiconductor with an energy gap E_g of about 300 meV.[12] The localized Tm^{2+} $4f^{13}$ level is situated within the energy gap between a filled anion *p* band and an empty cation $5d6s$ conduction band. The $5d$ band is crystal-field split into the upper $5de_g$ and the lower $5dt_{2g}$ branch; the bottom of the latter lies below the bottom of the $6s$ band.[13-15] The relevant energy gap E_g for $4f^{13}5d^0 \rightarrow 4f^{12}5d^1$ excitations is given by the separation of the $4f^{13}$ level from the bottom of the $5dt_{2g}$ bands. The exchange of more and more (large) Te^{2-} by (small) Se^{2-} leads to a reduction of the lattice constant. The consequence is an increase of the strength of the crystalline field which increases the separation of the $5dt_{2g}$ and the $5de_g$ subbands, leading to a decrease of the energy gap. In $TmSe_{0.60}Te_{0.40}$, E_g is reduced to about 40 meV.[12] The

Se-rich $TmSe_{1-x}Te_x$ compounds ($x<0.18$), on the other hand, are intermediate-valence metals.[12,16] The variation of stoichiometry does not lead to a continuous SMT, in the range $0.18<x<0.4$ there is a miscibility gap.[12,17]

The semiconducting compounds $TmSe_{1-x}Te_x$ ($0.4\leq x\leq 1$) can be transformed into a metallic state on the application of external pressure.[12,18,19] The SMT is continuous for $0.5\leq x\leq 1$, but discontinuous for $0.4\leq x<0.5$. Now it is the pressure which reduces the lattice constant and hence decreases, via crystalline-field splitting of the $5d$ band, the energy gap. Resistivity measurements at room temperature give clear evidence for the pressure-induced SMT.[12,18,19] Hall-effect data of $TmSe_{0.32}Te_{0.68}$ under pressure[12,18] indicate the conductivity to be mainly determined by the thermal excitation of localized $4f^{13}$ electrons into $4f^{12}5d^1$ bandlike states. The SMT involves a change in the valence of the Tm ions leading to a considerable volume collapse of the crystal and a negative Poisson's ratio.[18,20,21] The Tm ions are no longer divalent but *intermediate valent* between 2+ and 3+, where the degree of valence mixing is determined by $a|4f^n\rangle+b|4f^{n-1}5d^1\rangle$. Intermediate valency is indicated further by high-pressure investigations of susceptibility[12,18,20] and L-edge absorption.[22,23] The crystal structure remains NaCl type.[19]

The magnetic properties of $TmSe_{1-x}Te_x$ are of special interest since in this system a coexistence of intermediate valence and magnetic order occurs. Stoichiometric TmSe exhibits antiferromagnetism (type I) below $T_N\approx 3$ K.[24] But the type of order can easily be changed to *ferromagnetism* either through the application of a moderate magnetic field (3–4 kOe) (Ref. 24) or through the exchange of some Se by Te. Metallic $TmSe_{1-x}Te_x$ in the range $0.1\leq x\leq 0.18$ is ferromagnetic[16,20,25,26] with $T_C=1.8$–3.7 K. The semiconducting $TmSe_{1-x}Te_x$ compounds have a completely different magnetic behavior. They are antiferromagnets with very low ordering points: $0.4\leq x<1$, $T_N=0.2-0.3$ K (Ref. 12) and $x=0$ (TmTe), $T_N=0.2$–0.4 K (AF II).[27,28] Under pressure, however, they reveal a SMT which has significant implications on magnetic order. Wohlleben *et al.*[29] have found that at 30–50 kbar TmTe (metallic at these pressures) has an ordering point lying above liquid-helium temperature. And Batlogg *et al.*[30] showed that metallic pressed $TmSe_{0.60}Te_{0.40}$ can have the magnetic ordering point as high as 5.6 K.

With our low-temperature high-pressure study of semiconducting $TmSe_{1-x}Te_x$ compounds we want to investigate the SMT at low temperatures. Theoretical considerations predict the continuous SMT (at 300 K) to be first order at low temperatures.[31] Also the pressure-volume phase diagram of $TmSe_{1-x}Te_x$ (Ref. 12), which is reminiscent of the van der Waals gas, suggests a discontinuous behavior at low temperatures. We will show that this indeed is the case for $TmSe_{0.45}Te_{0.55}$. Furthermore, we have discovered a novel feature in the pressure dependence of the resistivity at low temperatures. A fascinating interpretation could be the transition to an excitonic insulator state. Finally, the evolution of magnetic order has been studied under pressure.

II. EXPERIMENTAL DETAILS

A. Pressure equipment

To perform high-pressure experiments we have used a CuBe clamp cell combined with the Teflon-cell technique. The pressure medium was 1:1 *n*-pentane-isoamyl alcohol. Pressures up to 18 kbar were generated and locked in at ambient temperature. The small size of the device (outer diameter, 25.4 mm; inner bore, 6 mm) allowed it to be introduced into a cryostat. The pressure has been determined in *in situ* by a manganin gauge, which was calibrated[32] with the first-order phase transition (I-II) of Bi occurring at 25.5 kbar.[33] During the cooling process of the CuBe cell the pressure medium freezes, but the pressure is thought to remain quasihydrostatic.[34] The pressure loss which comes along with the cooling could be determined accurately using the method described by Thompson.[34] In the transformation of the measured $\rho(T)$ curves (for various pressures) into $\rho(p)$ curves (for fixed temperatures) we have always taken into account the temperature dependence of pressure.

B. Samples

All our measurements have been performed on single-crystalline samples. The relevant data are provided in Table I. a_0 denotes the lattice constant at ambient conditions and No. is the specific number of the sample. The table also includes information about which measurement was performed on what sample.

C. Electrical resistivity

The electrical resistivity ρ has been measured with a four-probe method. We have used a lock-in technique with an alternating current of constant amplitude. The frequency was typically ~ 86 Hz. Assuming simple carrier statistics and a pinning of the chemical potential to the $4f$ level the resistivity of $TmSe_{1-x}Te_x$ in the semiconducting state becomes

$$\rho=\rho_0 e^{E_g/k_BT}. \tag{2.1}$$

TABLE I. Single-crystalline samples used in our experiments.

Substance	Batch	a_0 (Å)	No.	Volume (mm^3)	Measurements
$TmSe_{0.45}Te_{0.55}$	2142	6.137	4	$2.8\times1.3\times0.6$	$\rho(p,T,H),\chi(p,T)$
			5	$2.2\times2.2\times1.9$	neutrons,optics
$TmSe_{0.32}Te_{0.68}$	1799	6.21[a]	5	$2.2\times1.0\times0.5$	$\rho(\rho,T)$

[a]Reference 12.

Under pressure (at ambient temperature) an exponential decrease of the resistivity has been established up to the SMT where the resistivity becomes more or less pressure independent.[12,16,19,20] This implies through Eq. (2.1) a linear closing of the energy gap $E_g(p)$ under pressure p

$$E_g(p)=E_g(p=0)+p\frac{dE_g}{dp} , \tag{2.2}$$

when ρ_0 is taken to be pressure and temperature independent. E_g $(p=0)$ and dE_g/dp can be estimated from the resistivity-pressure curve. On the other hand, the energy gap can also be evaluated from a measurement of the temperature dependence of the resistivity. The slope of $\rho(T)$ in Eq. (2.1) in an Arrhenius plot ($\log_{10}\rho$ versus $1/T$) is determined by E_g.

D. Magnetic susceptibility

The magnetization M of a material depends on the internal magnetic field H_i. The *initial magnetic susceptibility* χ_{in} is defined as the slope of the $M(H_i)$ curve at zero internal field:

$$\chi_{in}\equiv\left.\frac{dM}{dH_i}\right|_{H_i=0} . \tag{2.3}$$

In the case of a ferromagnet χ_{in} is the slope of the *virgin curve* at $H_i=0$. χ_{in} of a material which magnetically orders has a marked structure at the ordering temperature. We have determined this temperature (in function of pressure) with a transformerlike arrangement containing the sample[35] introduced into the CuBe pressure cell. A primary coil generates via induction an ac-voltage in a secondary coil which contains the sample. Since the induced voltage depends on the sample's susceptibility, it's measurement gives information about the magnetic behavior. The signal was measured with a lock-in amplifier, the frequency being typically ~ 89 Hz.

Under the assumption of long and slim coils one finds for the relation between the measured signal (induced voltage V_{ind}) and the initial susceptibility χ_{in} the following formula (SI units):

$$V_{ind}=a_1\frac{1-N}{1/\chi_{in}+N}+a_2 . \tag{2.4}$$

N denotes the demagnetization factor. The coefficients a_1 and a_2 depend on the geometry and winding of the coils, on the volume of the sample, and on the current passing through the primary coil. a_2, the induced voltage in absence of any sample, could be reduced to small values if the secondary coil was made out of two *oppositely* wound subcoils. Equation (2.4) expresses the significant influence of the demagnetization factor on the measurement. The main temperature dependence of V_{ind} is due to $\chi_{in}(T)$ which reflects the nature of the magnetic behavior of the investigated material. Isotropic ferromagnets reveal a divergence of the magnetic susceptibility χ_{in} at the Curie temperature T_C, χ_{in} remaining very large below T_C. This makes via Eq. (2.4) V_{ind} flat below T_C and monotonically decreasing above T_C. At the ordering point itself a distinct kink is present. This has been found, for example, in EuO and EuS.[35] Hard ferromagnets, on the other hand, show below T_C a pronounced decrease of V_{ind} with decreasing temperature. This is due to the fact that in such materials χ_{in} (the slope of the virgin curve) can become very small as the coercive force H_c gets large:[36]

$$\chi_{in}=\text{const}\times\frac{1}{H_c} . \tag{2.5}$$

An example is USe.[37] In antiferromagnets the susceptibility is always finite and $\chi_{in}(T)$ shows a peak structure with the Néel temperature T_N lying on the low-temperature side of the peak. In fact, T_N coincides with the temperature where $\chi_{in}(T)$ has maximum slope.[38] This behavior is clearly seen in the antiferromagnet EuTe.[35]

E. Elastic neutron scattering

These experiments have been performed at the Saphir reactor in Würenlingen, Switzerland, in cooperation with the Laboratorium für Neutronenstreuung, Eidgenössische Technische Hochschule (ETH) Zürich.

We have used a double-axis spectrometer at a fixed neutron wavelength of $\lambda=2.35$ Å. The sample (angle ω), sitting in the neutron beam, and the detector (angle 2θ) could be rotated independently about a common vertical axis. Reciprocal space was probed, e.g., in the ω- or rocking-scan mode (only crystal is rotated), or in the 2:1-scan mode (both crystal and detector are rotated simultaneously).

Due to attenuation, only about 7% of the incident neutrons passed the CuBe pressure cell. Nevertheless we observed clear-cut Bragg reflections due to the sample. The experiment has been performed on single crystalline $TmSe_{0.45}Te_{0.55}$ sample 5 which had a volume of ~ 9 mm^3. The sample had faces of equivalent {100} planes. We put the crystal inside the pressure cell such that the (011) plane coincided with the scattering plane. This made it possible that all points (being close enough to the origin) in reciprocal space lying in the plane defined by [100] and [011] were accessible.

The $TmSe_{1-x}Te_x$ compounds crystallize in the NaCl structure. For a fcc lattice nuclear Bragg reflections *hkl* are, in principle, observable if all *hkl* are even or all are odd. However, the numerical evaluation[39] of the nuclear structure factors of the specific compound $TmSe_{0.45}Te_{0.55}$, reveals that the intensity of nuclear reflections with odd *hkl* (e.g., 111,311) is 3 orders of magnitude smaller than the intensity of those with even *hkl* (e.g., 200, 400, 220, 222). This has the consequence that in the absence of magnetic scattering only the latter reflections are measurable. If, however, there is an onset of magnetic order, the diffraction pattern changes. *Ferromagnetism* results in an additional intensity to all allowed nuclear reflections. In $TmSe_{0.45}Te_{0.55}$, e.g., the 111 reflection should become observable. In the presence of *antiferromagnetism* (AF) new reflections will occur. For a fcc lattice AF(I) will lead to the magnetic reflections 100 and 011, whereas AF(II) will lead to $\frac{1}{2}\frac{1}{2}\frac{1}{2}$ and $\frac{3}{2}\frac{1}{2}\frac{1}{2}$.

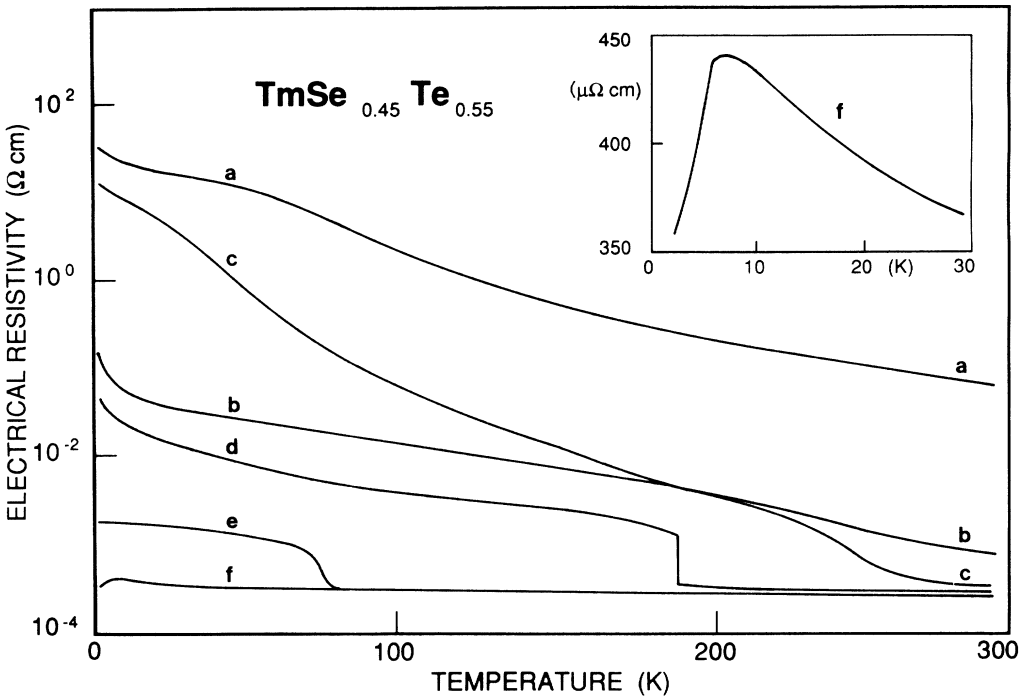

FIG. 1. Temperature dependence of the electrical resistivity of $TmSe_{0.45}Te_{0.55}$. The pressures at room temperature are $a=0$, $b=9.7$, $c=11.0$, $d=12.9$, $e=15.0$, and $f=17.0$ kbar, respectively. Note the linear scale for the resistivity in the inset. For clarity not all measured curves are shown.

F. Optics

Optical reflectivity has been measured at ambient pressure with two different apparatus covering the energy ranges 1–500 meV and 0.5–4.3 eV, respectively. The experiment has been performed at room temperature in the whole energy range, and at 6 K in the low-energy range. For the Raman scattering an argon ion laser was used. The incident wavelength was 514 nm. The scattered light was analyzed with the resolution of 1 meV. In the present study energy shifts from 0–185 meV were investigated.

III. RESULTS

A. Electrical resistivity

We have measured at *room temperature* the resistivities of $TmSe_{0.45}Te_{0.55}$ and $TmSe_{0.32}Te_{0.68}$ as a continuous function of pressure (Figs. 3 and 4, dashed lines). We observe an exponential decrease of resistivity which indicates according to Eq. (2.1) a linear closing of the energy gap under pressure [Eq. (2.2)]. As the resistivity becomes pressure independent, the gap is closed, and a *continuous* SMT has taken place. From our data we can estimate $dE_g/dp=-11.8$ and -13.0 meV/kbar, E_g $(p=0)=135$ and 185 meV, and the SMT taking place at 11.4 and 14.2 kbar for $TmSe_{0.45}Te_{0.55}$ and $TmSe_{0.32}Te_{0.68}$, respectively. These values compare well with measurements by Boppart.[12,20]

We then investigated the temperature dependence of resistivity of the same samples, being subjected to various pressures (Figs. 1 and 2). The *ambient pressure* curve of both (semiconducting) compounds reveals a resistivity increase from room temperature down to the lowest temperature (1.5 K) of about 3 orders of magnitude. The slope of the curve in the Arrhenius plot gradually decreases with decreasing temperature, which is probably

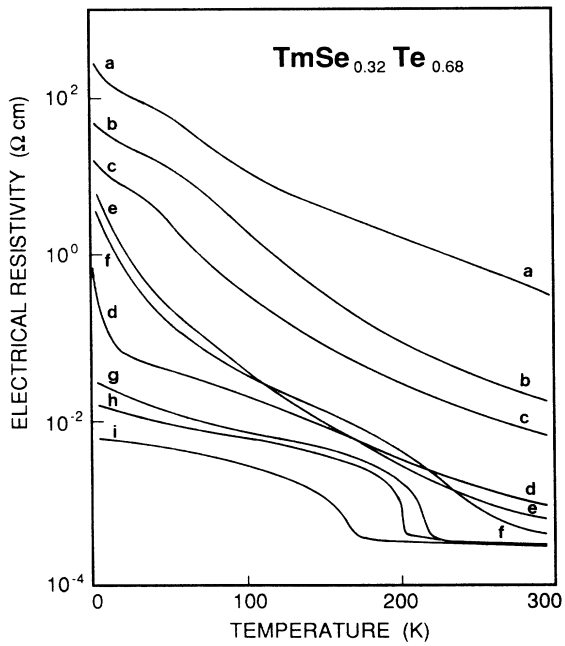

FIG. 2. Temperature dependence of the electrical resistivity of $TmSe_{0.32}Te_{0.68}$. The pressures at room temperature are $a=0$, $b=6.0$, $c=8.0$, $d=12.0$, $e=13.0$, $f=14.5$, $g=16.0$, $h=17.0$, and $i=18.0$ kbar, respectively. For clarity not all measured curves are shown.

due to extrinsic carriers. At room temperature the slope corresponds to [Eq. (2.1)] $E_g = 108$ and 156 meV for $TmSe_{0.45}Te_{0.55}$ and $TmSe_{0.32}Te_{0.68}$, respectively, being in reasonable agreement with the gap estimated from high-pressure data.

In order to study the influence of pressure, we have transformed all measured curves into a $\log_{10}\rho(p)$ plot, the temperature being a parameter (Figs. 3 and 4). It came as a surprise that for temperatures below about 250 K and most prominent at the lowest temperature (5 K in Figs. 3 and 4) the resistivity-pressure relations of $TmSe_{0.32}Te_{0.68}$ and $TmSe_{0.45}Te_{0.55}$ show a novel feature. After the initial decrease of resistivity, we observe, above a temperature and composition-dependent critical pressure, an *increase* of resistivity with increasing pressure, followed again by a decrease and a SMT. The lower the temperature the larger the increase of the resistivity. At 5 K the resistivity goes up by a factor of 370 for $TmSe_{0.45}Te_{0.55}$. In this pressure region the slope of the $\log_{10}\rho(p)$ curves is considerably increased on cooling, at 5 K we find $d\log_{10}\rho/dp \geq 2.5$ kbar^{-1} and even a first-order transition cannot be ruled out. For comparison, the rate of the resistivity decreases under pressure at room temperature $d\log_{10}\rho/dp \approx -0.2$ kbar^{-1} for the same sample.

The pressure-induced SMT cannot be studied directly at low temperatures with our CuBe clamp cell, since we cannot change the pressure at a fixed low temperature. Nevertheless, an indirect study is possible. In our experiments, the pressure cell is loaded at room temperature. On cooling, a certain amount of the pressure is lost which, however, we can measure accurately. Now, when we have driven the sample at room temperature slightly into the metallic state, the SMT can be reversed when the temperature is decreased. Depending on the initial pressure at room temperature, the SMT can be studied at various temperatures. This behavior is depicted in Fig. 5 for three different pressures for $TmSe_{0.45}Te_{0.55}$. While

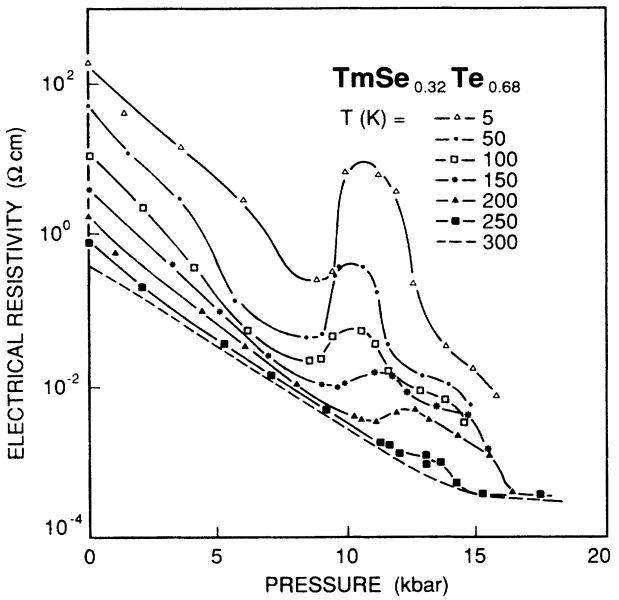

FIG. 4. Pressure dependence of the electrical resistivity of $TmSe_{0.32}Te_{0.68}$ for various temperatures. The thin solid lines are guides to the eye.

curve 1 shows a continuous transition, curve 2 exhibits a jump at 192 K and 11.0 kbar: the resistivity changes almost by a factor of 4 within less than 0.5 K (which causes a pressure change of less than 0.02 kbar). This clearly indicates a first-order SMT. For lower temperatures (curve 3) the transition is still quite sharp—it takes place over about 0.14 kbar—and we think that the discontinuous behavior is masked only by some nonhydrostatic behavior of the frozen pressure transmitting medium. We observe only a very small hysteresis $\Delta p \leq 0.04$ kbar which, however, is just about the experimental error. We would like to remark here that the hysteresis Δp of the

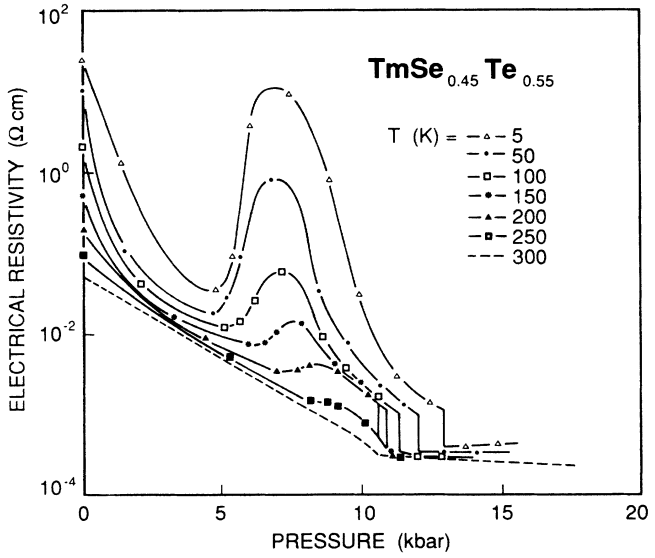

FIG. 3. Pressure dependence of the electrical resistivity of $TmSe_{0.45}Te_{0.55}$ for various temperatures. The thin solid lines are guides to the eye. For temperatures below 200 K a first-order SMT is suggested.

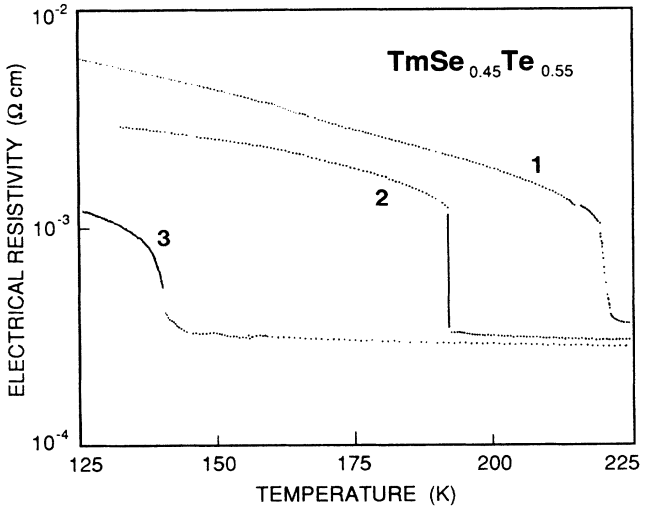

FIG. 5. Temperature dependence of the electrical resistivity of $TmSe_{0.45}Te_{0.55}$ for three different pressure runs. At room temperature the pressure is 12.0, 12.9, and 13.9 kbar and at the transition it is reduced to 10.7, 11.0, and 11.0 kbar for the curves 1, 2, and 3, respectively.

pressure-driven first-order SMT in $TmSe_{1-x}Te_x$ compounds is considerably smaller [$TmSe_{0.60}Te_{0.40}$: $\Delta p \approx 0.3$ kbar (Refs. 12 and 20)] than, for example, in $SmS_{1-x}Se_x$ compounds [e.g., SmS: $\Delta p \approx 5.7$ kbar (Ref. 40)]. The first-order SMT of $TmSe_{0.45}Te_{0.55}$ below ~200 K has been introduced into Fig. 3. The SMT in $TmSe_{0.32}Te_{0.68}$ seems to be continuous also at low temperatures.

At the highest pressures [Fig. 1, curve *f*: $p(5\text{ K}) = 14$ kbar], the compound $TmSe_{0.45}Te_{0.55}$ could be studied in the metallic state over the whole temperature range. The variation of resistivity with temperature is considerably smaller compared with the semiconducting state. We observe an increase of resistivity with decreasing temperature down to about 6 K, followed by a resistivity decrease.

Magnetoresistance has been studied on $TmSe_{0.45}Te_{0.55}$ under three different pressures (Fig. 6). In our experiments, both the current and the external magnetic field were parallel to the [100] direction. In Table II some values are compiled. The indicated pressures are the values of 4.2 K. ρ^0 denotes the resistance at $H = 0$; H_{max} is the applied magnetic field, where $\Delta\rho/\rho^0(H)$ has a maximum.

At 7.5 and 12.8 kbar the sample is in the semiconducting state, whereas at 15.2 kbar it is metallic. We observe in the metallic state a more pronounced magnetoresistance; and at low fields there is a distinct maximum. The field dependence of ρ is found to be the same for increasing and decreasing fields.

B. Magnetic susceptibility

The initial susceptibility χ_{in} of $TmSe_{0.45}Te_{0.55}$ has been measured via induced voltage [Eq. (2.4)] at four different pressures (Fig. 7). In the semiconducting state [p (5 K) = 8.5 and 13.6 kbar] there is only a slight increase of the susceptibility upon cooling. This is characteristic for paramagnetism. The magnetic ordering point lies well below 1.5 K. In the metallic state, on the other hand, there is a pronounced peak structure at T_{max} indicating the onset of magnetic order; $T_{max} = 5.8$ and 5.1 K for p (5 K) = 14.3 and 16.4 kbar, respectively.

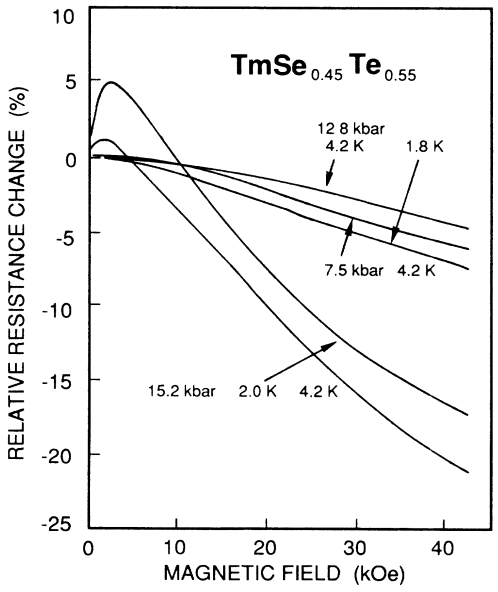

FIG. 6. Relative change of the electrical resistivity $\Delta\rho/\rho^0$ of $TmSe_{0.45}Te_{0.55}$ in function of magnetic field at various pressures and temperatures.

TABLE II. Magnetoresistance of $TmSe_{0.45}Te_{0.55}$ under pressure.

ρ (kbar)	T (K)	ρ^0 (Ω cm)	H_{max} (kOe)	$\Delta\rho/\rho^0$ (H_{max})	$\Delta\rho/\rho^0$ (43 kOe)
7.5	4.2	8.81	3.5	+0.1%	−6.3%
12.8	4.2	1.64×10^{-3}			−4.9%
	1.8	1.68×10^{-3}			−7.4%
15.2	4.2	4.45×10^{-4}	1.4	+1.3%	−20.9%
	2.0	4.01×10^{-4}	2.6	+4.9%	−17.1%

C. Neutron scattering

Neutron scattering has been performed on $TmSe_{0.45}Te_{0.55}$. Although faced with the problem of a small transparency of the CuBe pressure cell, we were lucky to find clear-cut Bragg reflections. It took somewhat more than an hour to perform one scan over a position in reciprocal space. A scan along a certain direction (e.g., from the origin to 022) took 6–13 h.

The observability of reflections has been discussed in Sec. II E. Three different pressure runs were realized.

1. p(300 K) = 11.9 kbar

At 10 K the pressure is reduced to 8.5 kbar. At this pressure the sample is in the state with the anomalously

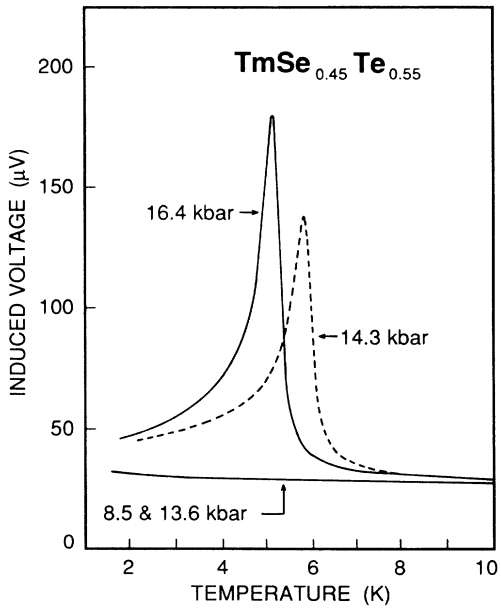

FIG. 7. Induced voltage V_{ind} (magnetic susceptibility) as a function of temperature of $TmSe_{0.45}Te_{0.55}$ for various pressures, whose magnitudes are indicated for $T = 5$ K. In the metallic state ($p = 14.3$ and 16.4 kbar) a pronounced peak structure can be observed, whereas in the semiconducting state ($p = 8.5$ and 13.6 kbar) the susceptibility remains very small.

enhanced resistivity. We made this experiment in order to look for a possible crystallographic phase transition which could be the cause for the resistance anomaly. We performed ω- and 2:1-scans at positions 200, 400, 220, 222, 111, 100, 011, and 211 in reciprocal space at temperatures 300 and 10 K. The reflections 200 and 400 have been measured in the whole temperature range 10–300 K. The fcc allowed nuclear Bragg reflections 200, 400, 220, and 222 could be observed very well. No other reflections were present and there was also no broadening of the nuclear Bragg reflections at 10 K with respect to 300 K. These findings indicate the *absence of a structural phase transition.* At room temperature the sample was in the metallic state with Tm being intermediate valent. Upon cooling, the SMT is reversed and Tm becomes more divalent, which increases the lattice constant a_0 considerably. From the neutron data it is possible to calculate a_0 via

$$a_0 = \frac{4\pi}{Q_{400} - Q_{200}} \,. \tag{3.1}$$

Q_{400}, Q_{200} are the lengths of the scattering vectors of the 400 and 200 Bragg reflection, respectively. Between 255–210 K the lattice constant increases by remarkably 1.6% (Fig. 8). Over this temperature range the pressure is reduced by about 0.8 kbar. To get the same change of the lattice constant at room temperature the pressure has to be changed by about 3 kbar.[20] This is further evidence that the valence transition goes towards first order at low temperatures. The observed change in a_0 (Fig. 8) is of the same order as the pressure-induced first-order change in lattice constant of $TmSe_{0.60}Te_{0.40}$ at room temperature.[12,20]

2. *p(300 K)=17.7 kbar*

At this pressure the sample was in the metallic state down to the lowest temperature [p(1.5 K)=15.0 kbar]. The purpose was now the study of magnetic order. We performed ω- and 2:1 scans at 10 and 1.5 K at positions 200, 400, 022 (nuclear), 111 (F), 100 (AF I), and $\frac{1}{2}\frac{1}{2}\frac{1}{2}, \frac{3}{2}\frac{1}{2}\frac{1}{2}$ (AF II). Furthermore we made at 1.5 K 2:1 scans in three directions in reciprocal space (in steps of 0.2° in 2θ): from the origin out to 200, 022 [including the AF(I) reflection 011], and 111. At 10 K only nuclear Bragg reflections were present in the diffraction pattern (Figs. 9 and 10). At 1.5 K, however, in addition to these we also observed the 111 reflection but no AF peaks. We conclude that the sample is *ferromagnetic* at low tempera-

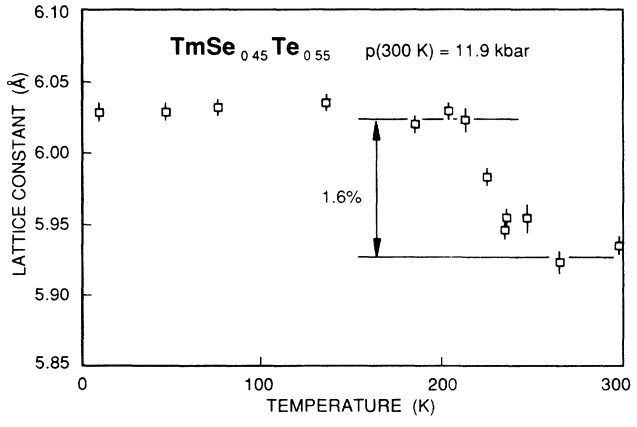

FIG. 8. Neutron scattering on $TmSe_{0.45}Te_{0.55}$ at p (300 K)=11.9 kbar. Temperature dependence of the lattice constant a_0. Below 255 K a_0 increases by 1.6% indicating the valence transition.

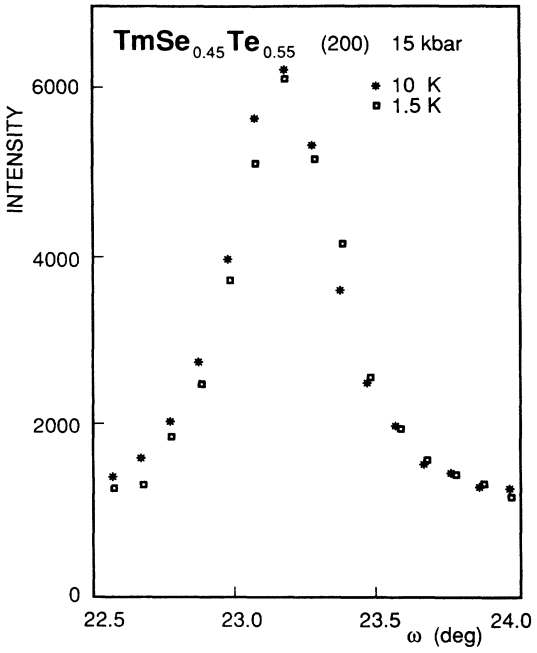

FIG. 9. Rocking scan of the 200 (nuclear) Bragg reflection of pressure-driven metallic $TmSe_{0.45}Te_{0.55}$ (p = 15 kbar).

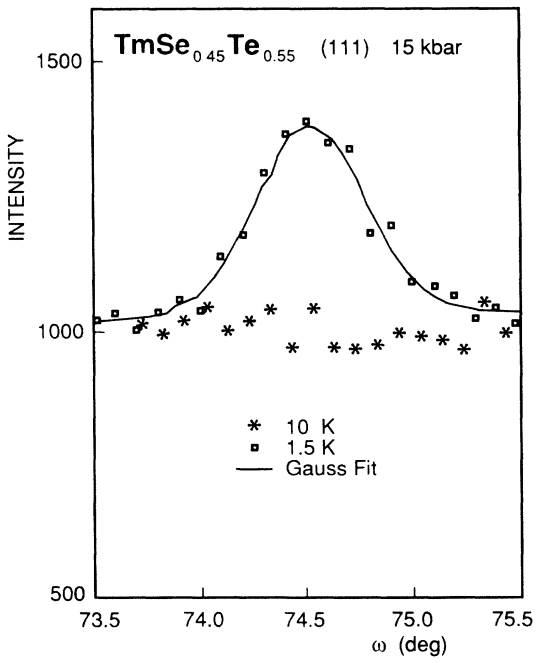

FIG. 10. Rocking scan of the 111 (ferromagnetic) Bragg reflection of pressure-driven metallic $TmSe_{0.45}Te_{0.55}$ (p = 15 kbar).

tures in zero external field. A comparison of the integrated neutron density of the 111 with the 200 peak yields the ordered moment μ_{Tm} of the Tm ions.[41] Using the magnetic form factor of the free Tm ion in the dipole approximation[42] we find $\mu_{Tm}=1.8\pm0.4\mu_B$ (at 1.5 K). We have also measured the temperature dependence of the maximum intensity of the 111 peak (Fig. 11). This yields the sublattice magnetization M. The data can be fitted astonishingly well with the power law

$$M \propto \varepsilon^{\beta}, \quad \text{where } \varepsilon \equiv \frac{T_C - T}{T_C} . \tag{3.2}$$

From this evaluation we derive the Curie temperature $T_C=5.07\pm0.1$ K and the critical exponent $\beta=0.32\pm0.03$ ($\varepsilon=0.002-0.3$). A last important result of the neutron scattering at this pressure is that the lattice constant $a_0=5.90\pm0.05$ Å at 2 K is significantly smaller than at ambient conditions (6.137 Å) indicating that the sample is indeed in the collapsed intermediate-valence phase. The variation of the temperature through T_C has no effect on the position of the nuclear Bragg reflections which proves that intermediate valency and magnetic order can coexist in this compound.

3. *p(300 K)=9.8 kbar*

This measurement was made to check the absence of magnetic peaks at 1.5 K ($p=5.8$ kbar) in the semiconducting state. At this temperature we performed ω- and 2:1-scans at positions 200, 400, 022 (nuclear), 111 (F), 100, 011 (AF I), and $\frac{1}{2}\frac{1}{2}\frac{1}{2}, \frac{3}{2}\frac{1}{2}\frac{1}{2}$ (AF II). Again 2:1 scans from the origin to the 200,111,022 Bragg reflections were made. Beside the nuclear reflections no other peaks were present proving the *absence of magnetic order.*

D. Optics

We have performed at ambient pressure optical-reflectivity measurements on $TmSe_{0.45}Te_{0.55}$ at 6 and 300 K in the energy range 1 meV–4.3 eV (Fig. 12). With the Kramers-Kronig analysis all optical constants could be derived.

The most obvious feature is a phonon structure around 16 meV. The increase of the reflectivity towards 1 meV at room temperature is due to the presence of thermally activated carriers. At 6 K they are frozen-out and hence the reflectivity levels off at the lowest energies and also the phonon structure becomes more pronounced with the maximum followed by a minimum. The energy gap is estimated from high-pressure resistivity data to be about 135 meV (Sec. III A). The imaginary part of the dielectric function (ϵ_2) reveals indeed the beginning of a structure around this energy. At about 60 meV, however, there is an additional structure. An analysis with Lorentz oscillators reveals it to lie at ~63 meV at 6 K and at ~57 meV at room temperature. We suggest this

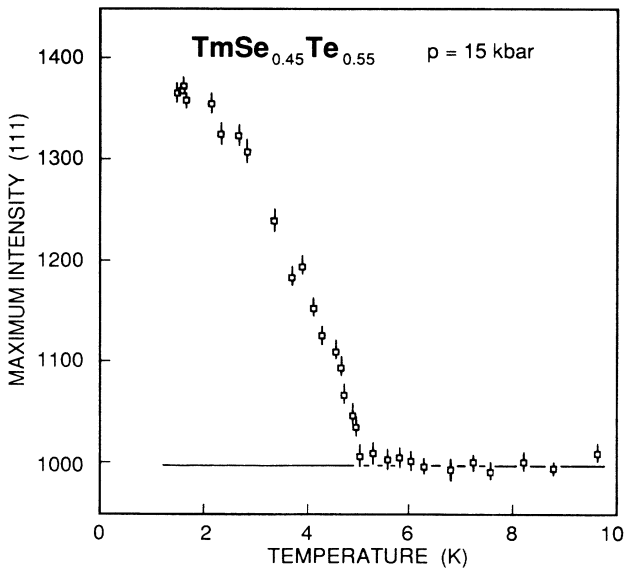

FIG. 11. Temperature dependence of the maximum intensity of the 111 reflection of $TmSe_{0.45}Te_{0.55}$ at $p(1.5\text{ K})=15$ kbar. The horizontal solid line represents the background. The intensity above the background is due to magnetic scattering, and is proportional to M^2.

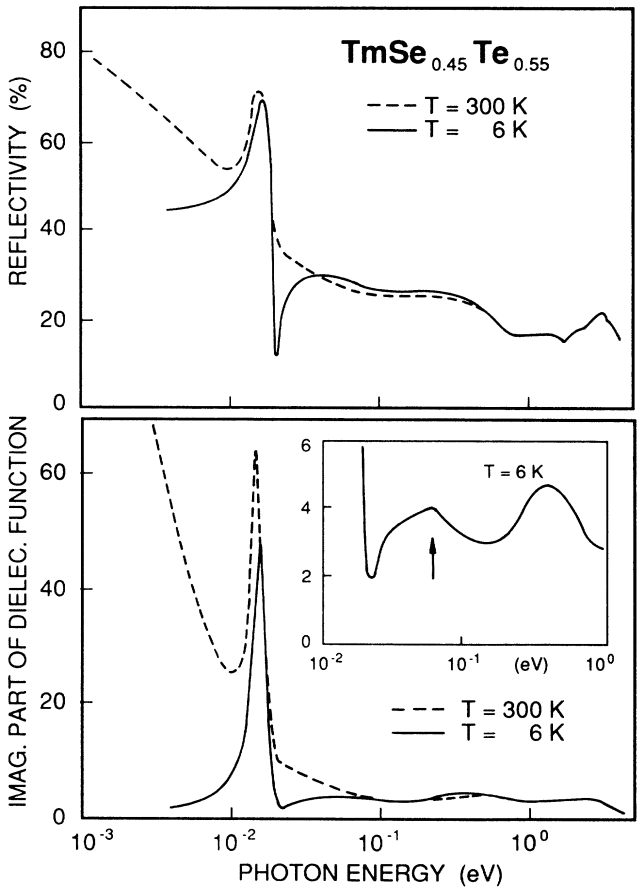

FIG. 12. Optical reflectivity (upper part) and imaginary part (ϵ_2) of the dielectric function (lower part) of $TmSe_{0.45}Te_{0.55}$ at $p=0$ kbar as a function of the photon energy. Solid lines, $T=6$ K; dashed lines; $T=300$ K. The structure in ϵ_2 at 60 meV (arrow in the inset) is suggested to be due to an exciton.

structure to be due to excitations of $4f$ electrons to an excitonic level lying below the $5d$ conduction band.

A Raman-scattering experiment has been performed on the same sample at $p=0$ in order to look for a structure near 60 meV. The spectrum has been investigated with energy shifts 0–125 meV (300 K) and 0–185 meV (50 K). Both spectra reveal at about 20 meV a peak which has been found in all semiconducting $TmSe_{1-x}Te_x$ compounds[43] and represents a weighted phonon density of states. Beside this structure we find no other peaks in $TmSe_{0.45}Te_{0.55}$. An explanation could be that the 60-meV phenomenon is infrared active but not Raman active. It would be informative to perform resonant Raman scattering where the incident laser beam energy is close to the gap energy (135 meV).

The absorption constant K can be deduced from the Kramers-Kronig analysis of the reflectivity spectrum. For $TmSe_{0.45}Te_{0.55}$ at 6 K we derive $K \approx 6000\ cm^{-1}$ at 60 meV. To get a transmission of a few tenths of a percent the crystal should be as thin as 10 μm which is not feasible with cleaving. Thinning by mechanical polishing, on the other hand, has to be avoided since it induces the valence transition on the surface. We think that the 60-meV phenomenon in $TmSe_{0.45}Te_{0.55}$ can be studied in *transmission* only on thin films of this material.

IV. DISCUSSION

A. Novel pressure-induced semiconductor-to-metal transition

The most fascinating feature of our high-pressure investigation of $TmSe_{1-x}Te_x$ compounds is without any doubt the unusual pressure dependence of resistivity at low temperatures (Figs. 3 and 4).

In a theoretical paper[31] a certain similarity of semiconducting $TmSe_{1-x}Te_x$ with expanded ScN has been suggested. Real ScN (Ref. 44) is a semimetal. Local density approximation, however, predict it to be a narrow (indirect) gap material.[31] Monnier *et al.*[45] have demonstrated that the electron-hole correlation effects play an important role in ScN. Taking into account these effects they could show that the electron-hole liquid (EHL) is the true ground state. Expanded ScN, on the other hand, is a semiconductor, which is expected to undergo a first-order transition to the EHL state as the lattice parameter is reduced. The transition of semiconducting expanded ScN to an excitonic insulator is ruled out[45] with the observation that for such indirect gap materials the binding energy per pair of the EHL is always larger than the binding energy of the free exciton. The argument is essentially based on the existence of *three* equivalent minima of the conduction band at the X point which reduces the kinetic energy of the EHL. Jansen *et al.*[15] have calculated the band structure of TmSe over a wide range of volumes, including the semiconducting state (negative pressure) and the metallic state (ambient pressure). Through the interaction with the ligand p orbitals (covalency) and hybridization with the d band (intermediate valency), the $4f$ bands acquire a finite curvature. The position of the $4f\Gamma_{15}$ level is much higher than one would extrapolate from the flat f bands in other parts of the Brillouin zone. Furthermore, in the semiconducting state, at the X point three degenerate minima of the conduction band occur. Subsequently Jansen *et al.*[31] have noticed that the band structure of semiconducting $TmSe_{1-x}Te_x$ in the neighborhood of the Fermi energy is close to that of expanded ScN. On the basis of this comparison they predict that the pressure-induced SMT of $TmSe_{1-x}Te_x$ which is continuous for $0.5 \le x \le 1$ should be discontinuous at low eneough temperatures.

Our resistivity measurements on $TmSe_{0.45}Te_{0.55}$ definitely show that the very transition from the semiconducting to the metallic state is discontinuous at low temperatures whereas at room temperature it is continuous (Figs. 3 and 5). The neutron-scattering data reveal the valence transition to take place over a considerably smaller pressure range at low temperature (Fig. 8) than at 300 K. And finally an abrupt SMT at about liquid-helium temperature is also indicated by the immediate onset of magnetic order as determined from susceptibility measurements (Fig. 7). These findings taken alone would support the above presented theoretical considerations. But if we look at the whole picture (Figs. 3 and 4) we perceive immediately that with increasing pressure there is not a simple transition from the normal semiconducting state to the metallic state but there is first a transition to a new, more insulating state. To our knowledge no other rare-earth compound has been found yet to show a similar effect.

One could imagine that the resistivity peak (Figs. 3 and 4) is due to magnetism. Our experiments on $TmSe_{0.45}Te_{0.55}$ under pressure tell us, however, that a magnetic field has only little influence on the resistivity peak height. It shall be mentioned in this context that SmS (Ref. 46) and TmSe (Refs. 47 and 48) show a considerable magnetoresistance. Furthermore we find the magnetic ordering temperature of $TmSe_{0.45}Te_{0.55}$ to be well below 1.5 K at the resistance peak. Since the peak structure of $\rho(p)$ can be seen already at temperatures as high as 250 K these experimental results make it unlikely that this phenomenon is due to magnetic interactions.

The neutron-diffraction data point to the absence of a structural phase transition which could have been another explanation of the resistance peak.

A fascinating interpretation[49] of the resistivity anomaly could be the onset of an *excitonic instability.* This idea shall be discussed in detail in the following section. In another section we shall present a simple model which describes, however, the temperature dependence of the resistivity peak heights astonishingly well. The root idea here is a reduced mobility of carriers in the lower bound of the conduction band.

1. Excitonic insulator

Imagine a semiconductor at $T=0$ having an indirect energy gap G. The minimum of the empty conduction band and the maximum of the filled valence band in reciprocal space shall be separated by $\mathbf{w}$. The promotion of a valence-band electron to the conduction band leaves a positive hole in the valence band. Via screened Coulomb interaction electron and hole can be bound (binding energy E_B) and hence form an exciton. The exciton is a sharp

excited state of the system. It is situated within the energy gap, E_B below the conduction band. In the Mott-Wannier limit the electron-hole pair is loosely bound (radius r_{Ex}) and it extends over many unit cells in real space. In this case holds[50]

$$E_B = \frac{\mu/m_0}{\epsilon^2} \times (13.6 \text{ eV}) , \tag{4.1}$$

$$r_{Ex} = \frac{\epsilon}{\mu/m_0} \times (0.53 \text{ Å}) , \tag{4.2}$$

ϵ denotes an appropriate dielectric constant, $\mu = (1/m_e + 1/m_h)^{-1}$ is the reduced mass of electron mass m_e and hole mass m_h, and m_0 is the mass of the free electron. Examples are Si and Ge with $E_B \approx 13$, ≈ 3 meV, and $r_{Ex} \approx 50$, ≈ 180 Å, respectively.[51] The Frenkel exciton, on the other hand, is fairly localized in real space and has a large binding energy. It represents essentially an excited state of a single atom. Solid krypton and KCl with $E_B \approx 1.5$ and ≈ 0.4 eV,[52] respectively, are examples of this type of exciton.

In the following discussion G shall denote the energy gap of an indirect semiconductor in the absence of electron-hole interaction. Let us assume a process (e.g., pressure, alloying) which reduces the energy gap G but retains the excitonic binding energy E_B. It has been suggested by Knox[53] in 1963 that as soon as $G < E_B$ the conventional insulating ground state would be unstable against the formation of excitons, and a transition to a new phase, which is called *excitonic insulator*[54] would result. Only if the gap G is reduced to a critical value G_c (usually $G_c < 0$) the material becomes a metal. Subsequently the theory of the new phase in the Mott-Wannier exciton limit was developed (e.g., des Cloizeaux,[55] Kozlov and Maksimov,[56] Keldysh and Kopaev,[57] Jérome *et al*,[54] and Halperin and Rice[58]). For a discussion we follow Ref. 54. We introduce creation and destruction operators: $a_{\mathbf{k}}^*, a_{\mathbf{k}}$ create and destroy electrons in the valence band with wave vector $\mathbf{k}$; $b_{\mathbf{k}}^*, b_{\mathbf{k}}$ create and destroy electrons in the conduction band with wave vector $\mathbf{w}+\mathbf{k}$. Then the conventional insulating ground state in the Hartree-Fock approximation is given by

$$\Phi = \prod_{\mathbf{k}} a_{\mathbf{k}}^* |\text{vac}\rangle , \tag{4.3}$$

where $|\text{vac}\rangle$ is the state with no electrons, and $\mathbf{k}$ runs over the Brillouin zone. The ground state of the excitonic insulator, however, is of the form

$$\Psi = \prod_{\mathbf{k}} \alpha_{\mathbf{k}}^* |\text{vac}\rangle , \tag{4.4}$$

where $\alpha_{\mathbf{k}}^*$ creates an electron in a linear combination of valence and conduction-band states,

$$\begin{aligned} &\alpha_{\mathbf{k}} = u_{\mathbf{k}} a_{\mathbf{k}} - v_{\mathbf{k}} b_{\mathbf{k}} , \\ &|u_{\mathbf{k}}|^2 + |v_{\mathbf{k}}|^2 = 1 . \end{aligned} \tag{4.5}$$

This represents a correlated mixing of valence- and conduction-band states. It has been found that in the excitonic insulator state the actual energy gap E_g is larger than the gap G (in absence of electron-hole interaction) according to

$$E_g = (G^2 + \Delta^2)^{1/2} . \tag{4.6}$$

Δ is the gap due to electron-hole correlation and has been calculated as a function of G.[56] The transition into the excitonic insulator state is predicted to be second order[54,56] or first order.[59,60] Due to the coupling of valence- and conduction-band states, which are separated by $\mathbf{w}$ in reciprocal space, a new periodicity $2\pi/|\mathbf{w}|$ occurs in the crystal.[58] This can result either in a charge-density wave (CDW) leading to a crystallographic distortion or in a spin-density wave (SDW) giving rise to antiferromagnetism.

The excitonic insulator occurs (at $T=0$) when $G = E_B$. For a loosely bound exciton $E_B \propto \epsilon^{-2}$ [Eq. (4.1)] Hence the excitonic insulator state can only exist if ϵ does not increase without any limit when the energy gap is reduced. ϵ, however, is expected to be roughly proportional E_d^{-2} (Ref. 58), where E_d is the *direct* energy gap. Since the direct gap is still large when the indirect gap G is closed, the situation $G = E_B$ seems to be realizable. The occurrence of a Mott-Wannier excitonic insulator phase has been questioned by Kübler.[61] He studied the dielectric screening of the electron-hole interaction for a simple (direct gap) band structure and found that the case considered does not become unstable toward exciton formation. Kübler[61] expects no essential change for an *indirect* semiconductor. In other words there are conflicting theories about the possible existence of the excitonic insulator. None of the existing theories, of course, is valid for a semiconductor with a valence band consisting of rather localized, (in function of pressure more and more) hybridized $4f$ states (narrow bands). We are left with the speculation that for more localized (Frenkel) excitons the screening of the Coulomb interaction is less effective and hence the excitonic insulator phase nevertheless can exist. This is supported by the study on expanded fluid mercury,[62] to be discussed below.

We would like to draw the attention now to the possible excitonic insulator behavior of $TmSe_{1-x}Te_x$ under pressure. In Fig. 13 a schematic $E(k)$ dispersion of semiconducting $TmSe_{1-x}Te_x$ at ambient pressure is drawn. The conduction band is the $5d$-derived $\Delta_{2'}$ band having its minimum at the X point. The "valence band" is

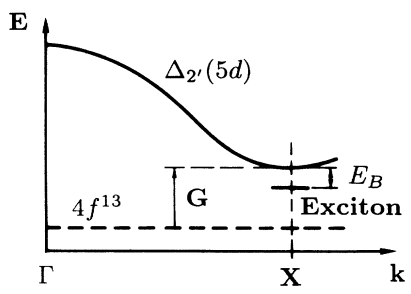

FIG. 13. Schematic $E(k)$ dispersion of semiconducting $TmSe_{1-x}Te_x$. G denotes the energy gap in absence of electron-hole interaction. Below the conduction-band minimum at the X point an excitonic level is assumed.

formed by the $4f$ states. G is the energy gap in absence of electron-hole interaction. We assume below the conduction band the existence of an exciton with binding energy E_B which shall be in first approximation independent of G. Let us look at our $\log_{10}\rho(p)$ curves for fixed temperature of $TmSe_{0.45}Te_{0.55}$ and $TmSe_{0.32}Te_{0.68}$ (Figs. 3 and 4). The initial decrease of ρ is due to the decrease of G. We speculate now that the point of the *increase of resistivity* with increasing pressure is the onset of an *excitonic instability*. The ground state is no longer a pure $4f^{13}$ state, but $5d$ conduction-band states get mixed in according to Eqs. (4.4) and (4.5). In other words, in the excitonic insulator state the $TmSe_{1-x}Te_x$ acquire a certain amount of intermediate valency. Within the framework of the above-mentioned theory the energy gap in the excitonic insulator is larger than in the absence of the electron-hole interaction [Eq. (4.6)]. Furthermore, in the excitonic insulator state not only have the ground-state ($4f^{13}$) conduction-band states mixed in, but also the excited states acquire a certain amount of valence-band ($4f$) character.[63] In our case this means that the carriers have a certain $4f$ character which reduces their mobility. Both effects tend to an increase of resistivity just as we observe in the experiment. Further increase of pressure reduces the gap again until finally a metallic state is realized in $TmSe_{1-x}Te_x$. These data can be interpreted as evidence for a *sequence of pressure-induced transitions from normal semiconductor to excitonic insulator to normal semimetal.*

What about the above-mentioned new periodicity $2\pi/|\mathbf{w}|$ which should be present in the excitonic insulator state? We have investigated the neutron-diffraction pattern of $TmSe_{0.45}Te_{0.55}$ at a pressure where the resistivity was enhanced, but found neither any new reflections nor a broadening of the fcc Bragg reflections, so there is no hint of any CDW or SDW. Also there is no anomaly in the susceptibility (under pressure) down to 1.5 K which could be due to a SDW. A SDW state may be detectable by its effect on nuclear magnetic resonance.[58] Several reasons could account for the absence of a new periodicity in our experiments. It is remarked in Ref. 58 that it is hard to detect this distortion, and if the exciton radius is more than a few lattice constants the magnitude of the distortion will be too small to be detected by neutrons or x rays. Another argument is based on the observation of Jansen *et al.*[15] that in $TmSe_{1-x}Te_x$ the $4f$ Γ_{15} level is pushed up in energy by interaction with the lower lying p states. According to these considerations, $TmSe_{1-x}Te_x$ could be termed *indirect* semiconductors with $|\mathbf{w}|=k_{\Gamma X}=2\pi/a_0$ (fcc lattice[52]). But this has the consequence that the new periodicity $2\pi/|\mathbf{w}|$ will be equal to the old lattice constant a_0 and no distortion of the lattice will occur. If, on the other hand, the $4f$ states are considered as completely localized, it is not clear whether any new periodicity in the excitonic insulator state should occur at all, since no $\mathbf{w}$ can be defined.

In Ref. 64 we find a qualitative phase diagram of the excitonic insulator in the temperature-gap ($T-G$) plane (Fig. 14). An essential feature of it is that at $T=0$ the excitonic instability occurs at $G=E_B$ but as the temperature is increased the instability occurs at $G<E_B$. The

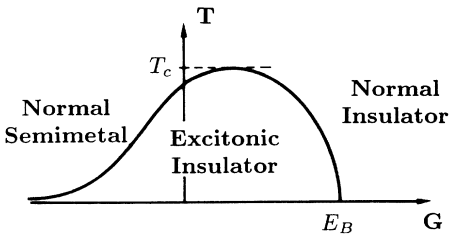

FIG. 14. Qualitative phase diagram of an excitonic insulator. $k_B T_c=\gamma E_B$, where γ is of order unity (after Ref. 64).

maximum transition temperature T_c is given by

$$k_B T_c=\gamma E_B \ , \tag{4.7}$$

where γ is of order unity. In order to compare our data with this phase diagram we make now the crude assumption that both dE_g/dp and E_g ($p=0$) of our compounds are temperature independent. This enables us to estimate the value of the (critical) energy gap E_g^c at the moment of the onset of the resistivity increase with increasing pressure (Figs. 3 and 4), in function of temperature (Fig. 15). Striking features of our data are first the near coincidence of the $T(E_g^c)$ relations of both $TmSe_{0.45}Te_{0.55}$ and $TmSe_{0.32}Te_{0.68}$, and second the surprising good agreement with the phase diagram of the excitonic insulator (Fig. 14). For $T\rightarrow 0$ we can deduce E_B, and taking $T_c=300$ K also $\gamma=k_B T_c/E_B$ can be estimated (Table III). We see that γ is really of the order unity and it compares well to $\gamma\approx 0.45$ taken in a theoretical work.[54] The magnitude of the binding energy of the exciton suggests them to be rather localized.

We have looked for an exciton in $TmSe_{0.45}Te_{0.55}$ at ambient pressure with optical means. The transition from the $4f$ level to the exciton should occur at $E_{ex}=E_g-E_B=(135-75)$ meV$=60$ meV. This is just the energy where we indeed observe in the Kramers-Kronig analyzed reflectivity spectrum a peak (Fig. 12). Thus the necessary presumption for the occurrence of an excitonic insulator, the presence of an exciton in the normal semi-

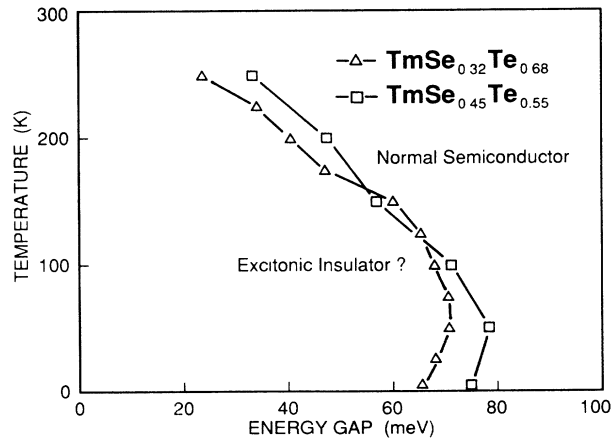

FIG. 15. Temperature dependence of the critical energy gap E_g^c represented in the T-G plane. We speculate that in the lower left part an excitonic insulator phase is present.

TABLE III. Excitonic insulator behavior of $TmSe_{1-x}Te_x$.

$TmSe_{1-x}Te_x$	x	E_B (meV)	γ
$TmSe_{0.45}Te_{0.55}$	0.55	75	0.33
$TmSe_{0.32}Te_{0.68}$	0.68	65	0.38

conducting state, might be fulfilled.

To our knowledge no material has been found up to now which shows without any doubt the transition to the excitonic insulator state. A promising candidate, however, seems to be $TiSe_2$.[65,66] This is a semimetal at ambient conditions with a very small negative gap (−50 meV) but at 200 K it exhibits a structural instability where the lattice constants are doubled. In the new state an energy gap occurs which is proposed[65] to be due to the realization of the excitonic insulator.

So far we have compared our data with existing theory of the Mott-Wannier–type excitonic insulator. If we evaluate the Mott-Wannier formula [Eq. (4.1)] for the excitonic binding energy with experimental data of $TmSe_{0.32}Te_{0.68}$ [$\mu \approx m_e \approx 9m_0$,[20] $\epsilon_{stat} \approx 10$, $\epsilon_{opt} \approx 6.7$ (Ref. 67)] we get unrealistically large values for E_B (more than 1 eV $\gg E_g$). This indicates that the excitons in $TmSe_{1-x}Te_x$ are rather localized, in which case Eq. (4.1) is not valid any more. The theory of the Frenkel excitonic insulator is not yet well developed. We would like to draw the attention now to two examples which are discussed in literature as excitonic insulators of the Frenkel type.

(a) Expanded fluid mercury (Hg). Turkevich and Cohen[62] suggest the occurrence of a Frenkel excitonic insulator in Hg. They have calculated the energy spectrum of Hg in function of the density ρ_{Hg}. At infinite dilution ($\rho_{Hg}=0$) the ground state is 6^1S_0, 6.7 eV above which a Frenkel exciton with $E_B=4.3$ eV exists. Increasing the density spreads the excitonic level into a band, the bottom of which comes down and finally at $\rho_{Hg} \approx 3$ g/cm^3 has the same energy as the 6^1S_0 level. At this density the binding energy of the exciton is only reduced to 3.7 eV. The normal insulating ground state, derived from the $6s^2$ atomic configurations, becomes unstable to condensation of Frenkel excitons. This point is experimentally identified with an anomaly in the dielectric constant. The new insulating ground state now possesses correlated $6s$-$6p$ mixing. Above a certain, higher density Hg then becomes a normal metallic liquid. The transition to the excitonic insulator state is expected to be first order and the $\rho_{Hg}-T$ phase diagram is predicted to be similar to the Mott-Wannier case.

(b) Alkali-doped rare-gas solids (e.g., Na in Ar, Kr, or Xe solids). This Frenkel excitonic insulator has been proposed by Logan.[63] At low-impurity concentration there is no impurity-impurity interaction so that there are sharp alkali levels. The Hamiltonian takes the form

$$\mathcal{H}=\mathcal{H}_0+\mathcal{H}_{int}+\mathcal{H}_{RG} \ . \tag{4.8}$$

Here $\mathcal{H}_0$ is the electronic Hamiltonian for the free alkali atom, $\mathcal{H}_{RG}$ is the Hamiltonian depending solely on the rare-gas atom's degrees of freedom, and $\mathcal{H}_{int}$ describes the coupling of the degrees of freedom of the impurity atom to those of the rare-gas atoms. The calculations of Logan suggest that there is a critical density ρ_{RG}^c of the rare-gas solid such that for $\rho_{RG} < \rho_{RG}^c$ the material is in the normal insulating domain in which the impurity electronic ground state is a spherically symmetric s state. For $\rho_{RG} > \rho_{RG}^c$, however, there is an excitonic insulator phase in which the impurity atoms possess electric dipole moments due to a sp hybridized ground state. In the excitonic insulator the energy difference between ground state and first excited state is increased with respect to the normal insulator.

Is it possible at all that in $TmSe_{1-x}Te_x$ there occurs a transition to the excitonic insulator? As mentioned above, in expanded ScN this transition is ruled out[45] with the observation that three *degenerate* conduction-band minima exist. Considering the similar band structure[31] the same argument would hold for $TmSe_{1-x}Te_x$. However, in the latter compounds each Tm ion has a statistically different anion surrounding. The resulting different ligand field splitting influences the bottom of the conduction band which appears somewhat warped. This mechanism has been proposed[16,20] to explain a change in slope of $\log_{10}\rho(p)$ curves (at 300 K) of $TmSe_{1-x}Te_x$ at higher pressures. The warping of the conduction band could remove the degeneracy of the three conduction-band minima at the X point and hence increase the kinetic energy of the electron-hole liquid (EHL) ground state. This favors the transition to the excitonic insulator.

2. Change of mobility

In this section we propose a simple model for the quantitative analysis of the temperature dependence of the peak heights of the measured resistivity-pressure curves of $TmSe_{0.45}Te_{0.55}$ (Fig. 3) and $TmSe_{0.32}Te_{0.68}$ (Fig. 4). The electrical transport shall be described in terms of an effective mass m^* (i.e., parabolic band) and a mobility μ of the conduction-band electrons. We start from the normal semiconducting state at $p=0$ (Fig. 16, left-hand side). We assume the following scenario. At a fixed temperature T, for $p>0$ the conduction band moves downward in energy (relative to the $4f$ level) initially without any change of its shape (m^* remains constant). In this pressure regime we observe the usual decrease of resistivity with increasing pressure. For higher pressures, howev-

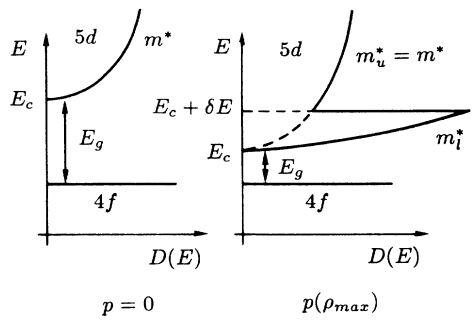

FIG. 16. Evolution of the energy levels of semiconducting $TmSe_{1-x}Te_x$ under pressure within the framework of the model discussed in this section.

er, there is an increase of resistivity, which in the present model shall be ascribed to the onset of distortion of the bottom of the conduction band. The energy gap shall *not* be influenced by this process. One could imagine the excitonic instability to be the trigger of such a rearrangement of the energy spectrum. On the other hand, it could also be the effect of the onset of a usual *f-d* hybridization due to the reduced magnitude of the energy gap E_g. We discuss the new state at the point of maximum resistivity.

Electrons in the lower part of the conduction band (from the bottom of the band at E_c to $E_c+\delta E$), due to the admixture of f character, shall have a reduced mobility μ_l and an enhanced effective mass m_l^* (index l for *lower*) (Fig. 16, right-hand side). At higher energies ($E>E_c+\delta E$) the corresponding values shall be μ_u and m_u^* (index u for *upper*), which we take to be equal to the values at $p=0$ (μ and m^*). $m_l^* \gg m_u^*$ leads to a peak structure in the density of states $D(E)$ for $E_c<E<E_c+\delta E$. We take δE to be temperature independent. The conductivity σ can be expressed as

$$\sigma=n_l q_e \mu_l + n_u q_e \mu_u \ . \tag{4.9}$$

q_e denotes the charge of the electron. n_l and n_u are the number of thermally activated electrons into the lower and upper part of the conduction band

$$n_l=2\int_{E_c}^{E_c+\delta E} D_l(E)F(E)dE \ , \tag{4.10}$$

$$n_u=2\int_{E_c+\delta E}^{\infty} D_u(E)F(E)dE \ , \tag{4.11}$$

where $D_{l,u}$ is the density of states and $F(E)$ is the Fermi distribution:[68]

$$D_{l,u}=\frac{1}{4\pi^2}\left[\frac{2m_{l,u}^*}{\hbar^2}\right]^{3/2}(E-E_c)^{1/2} \ , \tag{4.12}$$

$$F(E)=\frac{1}{e^{(E-\zeta)/k_BT}+1} \tag{4.13}$$

with ζ denoting the *chemical potential.* In the following we will assume the chemical potential to lie in such a way in the energy gap as to allow the approximation of the Fermi function $F(E)$ by the Boltzmann function $B(E)$

$$B(E)=e^{-(E-\zeta)/k_BT} \ . \tag{4.14}$$

If we introduce Eqs. (4.14) and (4.12) into Eqs. (4.10) and (4.11) we get for the number of electrons in the two different parts of the conduction band

$$n_l=2\frac{1}{4\pi^2}\left[\frac{2m_l^*}{\hbar^2}\right]^{3/2} e^{-(E_c-\zeta)/k_BT}(k_BT)^{3/2} \times\gamma(\tfrac{3}{2},\delta E/k_BT) \ , \tag{4.15}$$

$$n_u=2\frac{1}{4\pi^2}\left[\frac{2m_u^*}{\hbar^2}\right]^{3/2} e^{-(E_c-\zeta)/k_BT}(k_BT)^{3/2} \times\Gamma(\tfrac{3}{2},\delta E/k_BT) \ , \tag{4.16}$$

where γ and Γ are the *incomplete gamma functions*[69] which are defined as

$$\gamma(a,x)\equiv\int_0^x e^{-t}t^{a-1}dt \ , \tag{4.17}$$

$$\Gamma(a,x)\equiv\int_x^{\infty} e^{-t}t^{a-1}dt \ . \tag{4.18}$$

We now make the definition

$$\eta\equiv\frac{m_l^{*3/2}\mu_l}{m_u^{*3/2}\mu_u} \ . \tag{4.19}$$

η describes how different the lower and upper part of the conduction band are. $\eta=1$ means that they are equal. We will see that it is useful to introduce a new function

$$A(\delta E/k_BT,\eta)\equiv\eta+(1-\eta)\frac{\Gamma(\frac{3}{2},\delta E/k_BT)}{\sqrt{\pi}/2} \ . \tag{4.20}$$

A is a monotonic function of the argument $\delta E/k_BT$ and has the extrema $A=1$ for $\delta E/k_BT\to 0$ and $A=\eta$ for $\delta E/k_BT\to\infty$, respectively. $A\equiv 1$ for $\eta=1$. If we introduce Eqs. (4.15) and (4.16) and Eq. (4.9), and apply Eqs. (4.19) and (4.20) we derive the conductivity

$$\sigma=\frac{1}{4\pi^2}\left[\frac{2}{\hbar^2}k_BTm_u^*\right]^{3/2} q_e\sqrt{\pi}\mu_u e^{-(E_c-\zeta)k_BT} \times A(\delta E/k_BT,\eta) \ . \tag{4.21}$$

The absence of any distortion of the conduction band is equivalent to $\delta E=0$ or $\eta=1$. In both cases $A=1$, hence we define the *normal conductivity*

$$\sigma_{\text{norm}}=\frac{1}{4\pi^2}\left[\frac{2}{\hbar^2}k_BTm_u^*\right]^{3/2} q_e\sqrt{\pi}\mu_u e^{-(E_c-\zeta)/k_BT} \ , \tag{4.22}$$

and we can write for the conductivity

$$\sigma=\sigma_{\text{norm}}A(\delta E/k_BT,\eta) \ . \tag{4.23}$$

The effect of the admixture of f character to the d band is represented entirely by the function $A(\delta E/k_BT,\eta)$. To compare this result with the experiment we proceed as follows. We change to resistivities

$$\rho=1/\sigma \ , \qquad \rho_{\text{norm}}=1/\sigma_{\text{norm}} \tag{4.24}$$

and take the logarithm

$$\log_{10}\rho=\log_{10}\rho_{\text{norm}}-\log_{10}A(\delta E/k_BT,\eta) \ . \tag{4.25}$$

Let us look now at the experimental $\log_{10}\rho(p)$ curves for fixed temperatures (Figs. 3 and 4). With our model we intend to describe the height $\Delta\log_{10}\rho$ of the resistivity anomaly above extrapolated values from above and below the $\log_{10}\rho(p)$ peak. $\Delta\log_{10}\rho(T)$ is plotted in Fig. 17. We identify now

$$\Delta\log_{10}\rho(T):=\log_{10}\rho-\log_{10}\rho_{\text{norm}} =-\log_{10}A(\delta E/k_BT,\eta) \ . \tag{4.26}$$

In this analysis it is assumed that the chemical potential does not change when η becomes different from one. δE and η are assumed to be temperature independent and are treated as fit parameters such as to give the best rep-

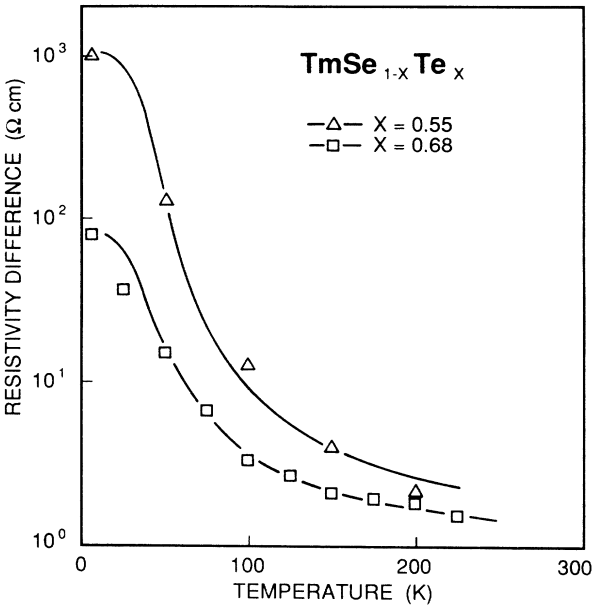

FIG. 17. Temperature dependence of the resistivity peak heights (Figs. 3 and 4) above extrapolated values from above and below the peak. Open symbols are measured values for $TmSe_{0.45}Te_{0.55}$ and $TmSe_{0.32}Te_{0.68}$ and the solid lines represent the model calculations as described in the text.

resentation of the experimental $\Delta\log_{10}\rho(T)$ data. The model parameters are collected in Table IV. The theoretical curve with these parameters follows the experimental data astonishingly well (Fig. 17). The values of δE are of a reasonable magnitude. For the interpretation of the η values it is instructive to look at the case where the mobility is dominated by the scattering of the carriers by thermal vibrations of the ions, then $\mu \propto m^{*-5/2}$ (Ref. 70). Introducing this relation into Eq. (4.19) we get $\eta = m_u^*/m_l^*$. Since we find $\eta \ll 1$ this would imply the effective mass to have high values in the lowest part of the conduction band, which means a considerable enhancement of the density of states.

This simple two-parameter model gives a reasonable well description of the peak heights of $\log_{10}\rho(p)$ as a function of temperature. We have assumed in this model that in the normal semiconducting state at low pressures $\delta E = 0$, and that at the maximum of the resistivity δE has the above-mentioned magnitude for the two $TmSe_{1-x}Te_x$ compounds. The detailed structure of the $\log_{10}\rho(p)$ curves is *not* explained and we think that the introduction of a pressure dependence of δE and η would not bring any further insight. A more realistic model should take into account also an increase of the energy gap, as it is predicted by the excitonic insulator model. If one wants to make the calculations with the Fermi function,

TABLE IV. Model parameters of $TmSe_{1-x}Te_x$.

$TmSe_{1-x}Te_x$	x	δE (meV)	η
$TmSe_{0.45}Te_{0.55}$	0.55	26	1×10^{-3}
$TmSe_{0.32}Te_{0.68}$	0.68	17	13×10^{-3}

the knowledge of the exact position of the chemical position is required.

B. Magnetism under pressure

Susceptiblity and neutron-scattering experiments on $TmSe_{0.45}Te_{0.55}$ indicate that the magnetic ordering point is well below 1.5 K when the sample is in the semiconducting state. In the pressure-induced metallic state, however, the ordering point is significantly enhanced and reaches nearly 6 K. Similar results have been found for the SMT in TmTe (Ref. 29) and $TmSe_{0.60}Te_{0.40}$ (Ref. 30). With neutron-scattering experiments we could prove that in pressure-driven metallic $TmSe_{0.45}Te_{0.55}$ magnetic order and intermediate valence can coexist.

It is an open question, why semiconducting $TmSe_{1-x}Te_x$ have such a low-ordering temperature ($T_N < 0.4$ K). TmSe has an appreciable ordered moment [$2.3\mu_B$ (Ref. 28)] and on the basis of the exchange mechanism discussed for the Eu chalcogenides, one would expect[71] it to be a *high* Néel temperature antiferromagnet. Instead T_N is below 0.4 K.[27,28] The considerable enhancement of the ordering temperature in the metallic state could be due to a qualitative change in the exchange mechanism. Whereas in the semiconducting state a *virtual f-d-f* exchange is effective, in the metallic state a *real* exchange occurs. The presence of free carriers could give rise to Ruderman-Kittel-Kasuya-Yosida (RKKY) interaction. On the other hand, in the metallic state the Tm ions are intermediate valent, and Varma[72] has proposed for this situation that the double exchange mechanism could play an important role.

In the vicinity of the Curie temperature, a *ferromagnetic metal* exhibits a decreasing resistivity with decreasing temperature.[73] If we compare resistivity (Fig. 1) and susceptibility (Fig. 7) data we find this characteristic of a ferromagnet to be present in intermediate valence metallic $TmSe_{0.45}Te_{0.55}$. Furthermore, there is a striking similarity of the temperature dependence of the resistivity of $TmSe_{0.45}Te_{0.55}$ in the metallic state (Fig. 1) with $TmSe_{0.83}Te_{0.17}$ (Ref. 25) and TmSe in a magnetic field ($H = 10$ kOe),[48] which both exhibit ferromagnetic order. These findings suggest that *ferromagnetism* is also present in metallic $TmSe_{0.45}Te_{0.55}$. This supposition is finally proved by our neutron-scattering data. The ordered moment (at 1.5 K) of the Tm ions amounts to $\mu_{Tm} = 1.8\mu_B$. This moment is far below the free-ion values of $4\mu_B$ and $7\mu_B$ for Tm^{2+} and Tm^{3+} but is comparable to the corresponding values of TmSe [$1.7\mu_B$,[24] $1.9\mu_B$ (Ref. 74)] and TmTe [$2.3\mu_B$ (Ref. 28)]. In the ferromagnetic metallic compounds $TmSe_{1-x}Te_x$ with $0.1 \le x \le 0.18$ the moment $\mu_{Tm} \le 1.6\mu_B$.[20,26]

Possible reasons for the reduced magnitude of the magnetic moments shall be briefly discussed. In the case of the metallic compounds one could imagine that the valence instability reduces the magnetic moment. This has been proposed for TmSe (Ref. 24) which is reported[24,75] to have no appreciable crystal electric-field (CEF) splitting of the $4f$ level. In pure TmTe, however, Tm is strictly divalent, hence the reduced moment cannot be explained by valence instability. But, a study of several

thermal properties of TmTe has shown CEF effects.[75] The Tm^{2+} ($J=\frac{7}{2}$) multiplet degeneracy is removed by the cubic CEF and the ground state is formed by a Γ_8 quartet. The two other excited states are doublets Γ_6 and Γ_7, respectively. The energy-level scheme Γ_8 (0 K)$-\Gamma_7$ (10 K)$-\Gamma_6$ (16 K) has been proposed.[75] The state Γ_8 has theoretically a saturated moment of $2.10\mu_B$. This value agrees reasonably with the measured magnetic moment of TmTe in the ordered state [$2.3\mu_B$ (Ref. 28)].

The shape of the susceptibility curve of pressure-driven metallic $TmSe_{0.45}Te_{0.55}$ (Fig. 7) is similar to those of $TmSe_{0.60}Te_{0.40}$ under pressure[30] and ferromagnetic $TmSe_{0.83}Te_{0.17}$ at $p=0$.[20,26] The peak structure could point to antiferromagnetic correlations. Although any *long-range order* of this type is excluded by our neutron-diffraction data. However, antiferromagnetic *short-range order* is still possible. On the other hand, Tm has a nonvanishing orbital moment, which destroys isotropy leading to some coercive force H_c. As discussed in Sec. II D the occurrence of $H_c \neq 0$ leads to a reduction of the susceptibility below T_C, giving rise to another explanation of the peak structure.

The temperature dependence of the sublattice magnetization M of ferromagnetic $TmSe_{0.45}Te_{0.55}$ obeys for $T<T_C$ a power law with the critical exponent $\beta=0.32\pm0.03$. Many magnetic materials have a β of such a magnitude [0.33–0.37 (Ref. 76)], which is definitely different from the mean-field value $\beta=0.5$. The theory indicates $\beta=0.325$ for the three-dimensional (3D) Ising systems, $\beta=0.345$ for the 3D XY model and $\beta=0.365$ for the 3D Heisenberg case.[77] Although the measured value of β favors the 3D Ising model, we think that a definite decision for a specific model cannot be made. The error bar of β represents just an estimate based on various fits. Above T_C a slight tail in the magnetization is indicated by our data (Fig. 11). Although the magnitude is less than the error bar, the fact that for four successive temperatures above T_C the magnetization is nonvanishing, makes the phenomenon plausible. One explanation is the existence of spin fluctuations. Part of the tail could also be due to the combined effect of the pressure dependence of T_C and a certain nonhydrostatic behavior of the pressure transmitting medium.

Let's look now at the *longitudinal magnetoresistance* of $TmSe_{0.45}Te_{0.55}$ (Fig. 6). We have found the magnetoresistance to be predominantly negative, which we attribute to an enhancement of the carrier mobility. The alignment of the magnetic moments of the Tm ions by the field leads to a reduction of the magnetic scattering. Because in the metallic state the measurement was performed below the ordering temperature, the change of the degree of alignment by the field is larger than in the paramagnetic, semiconducting state. This could be an explanation for the larger magnitude of the relative resistance change observed in the metallic state. Under these conditions the magnetoresistance of $TmSe_{0.45}Te_{0.55}$ is of comparable magnitude as observed in metallic (at $p=0$) $TmSe_{0.83}Te_{0.17}$ and $TmSe_{0.91}Te_{0.09}$ (Ref. 16). Astonishingly, we find in pressure-driven metallic $TmSe_{0.45}Te_{0.55}$ at low fields ($H<3$ kOe) a pronounced *positive* magnetoresistance. A similar effect has been reported[75] for TmSe ($\Delta\rho/\rho^0=+5\%$ at $H=1.2$ kOe and $T=1.45$ K). In other investigations[16,47] of TmSe this phenomenon, however, is absent. The nature of the positve magnetoresistance remains to be unraveled.

We will close this section with a brief discussion of the questions concerning the hybridization gap in pressure-driven metallic $TmSe_{1-x}Te_x$. Antiferromagnetic TmSe is known to have such a gap[78] and accordingly the resistivity steeply increases with decreasing temperature below T_N.[47,48] However, as the material is made ferromagnetic (magnetic field or substitution of Se by Te) the gap is absent for $T<T_C$ (Ref. 78) and the resistivity decreases for $T\rightarrow 0$.[16,47,48] Since in pressure-driven metallic $TmSe_{0.45}Te_{0.55}$ we also observe a decrease of resistivity with decreasing temperature below 6 K (Fig. 1), we conclude that in the ferromagnetically ordered state no gap is present. The situation is different in the paramagnetic state. Point-contact spectroscopy data[78] suggest a gap in $TmSe_{0.82}Te_{0.18}$ for $T>T_C$; this is compatible with the experimental observation of $d\rho/dT<0$ above T_C.[16] Pressure-driven metallic $TmSe_{0.45}Te_{0.55}$ shows also $d\rho/dT<0$ in the paramagnetic state (Fig. 1), this might be the result of an energy gap.

V. CONCLUDING REMARKS

In this study we have investigated the pseudobinary alloy system $TmSe_{1-x}Te_x$. These compounds exhibit a pressure-induced SMT coupled with a valence change. The SMT is well known in rare-earth monochalcogenides[19] and experimentally one observes in these materials a steady, exponential decrease of resistivty under pressure. We find the same behavior in our materials at room temperature. It came as a surprise, when we studied this transition in $TmSe_{0.45}Te_{0.55}$ and $TmSe_{0.32}Te_{0.68}$ at *low temperatures,* that these compounds reveal a *peak structure* in their $\rho(p)$ curves. We think that the proposed interpretations involving the concept of an excitonic insulator or the change of the mobility of carriers are very promising and should be further pursued. However, stressing the similarity[31] to the band structure of expanded ScN, a transition of semiconducting $TmSe_{1-x}Te_x$ to the excitonic insulator state should *not* occur. This argument is essentially based on the existence of three *degenerate* conduction-band minima. In $TmSe_{1-x}Te_x$, however, each Tm ion has a statistically different anion surrounding. We think that this deviation from full translational symmetry of the crystal might lift the degeneracy, leading to a single nondegenerate conduction-band minimum. In this case the excitonic instability is not ruled out any more, especially not when the valence band is a hybridized $4f$ state. It is an intriguing question, whether other compounds reveal a similar peak structure in $\rho(p)$ as is present in $TmSe_{1-x}Te_x$. We did not find evidence for this in $Tm_{0.5}Eu_{0.5}Se$ nor in $SmS_{0.89}Se_{0.11}$.[37] We believe, however, that the $SmS_{1-x}Se_x$ alloys are very promising candidates. One should investigate there especially the Se-rich stoichiometries, since they have a SMT which is first order of reduced strength or is continuous. Under these conditions the transition to the excitonic in-

sulator phase appears to be more probable.[58] The theory of the excitonic insulator has been developed predominantly for simple band structures with Mott-Wannier excitons. Our materials are much more complicated, however. In $TmSe_{1-x}Te_x$ the valence "band" is predominantly derived from localized $4f$ states and the excitons are probably of the Frenkel type; the development of a theory for the excitonic insulator taking into account these characteristics would be very desirable.

It remains an unresolved question, why the semiconducting $TmSe_{1-x}Te_x$ compounds have such a low ordering point ($T_N < 0.4$ K), although the Tm ions have an appreciable ordered moment [TmTe: $2.3\mu_B$ (Ref. 28)]. In the metallic state (achieved by pressure or stoichiometry) ferromagnetism with T_C up to 6 K occurs. We suspect the RKKY interaction and the double-exchange mechanism to play an important role in the enhancement of the ordering temperature.

ACKNOWLEDGMENTS

The authors wish to thank E. Kaldis for the preparation and chemical characterization of the single crystals. The help of W. Bührer, P. Fischer, and B. Hälg in the neutron-scattering experiments and W. Basca and F. Marabelli in the optical investigations is gratefully acknowledged. It is a pleasure to recall valuable discussions with W. Baltensperger, B. Bucher, M. Elmiger, R. Monnier, S. Schmitt-Rink, J. Schoenes, M. Solanki, and C. M. Varma. We are grateful for the technical support by J. Müller and H. P. Staub.

*Present address: Max-Planck-Institut für Festkörperforschung, Hochfeld-Magnetlabor, Centre National de la Recherche Scientifique (CNRS), Boîte Postale 166X, 38042 Grenoble CEDEX, France.

[1]B. Batlogg, E. Kaldis, A. Schlegel, G. von Schulthess, and P. Wachter, Solid State Commun. **19**, 673 (1976).
[2]C. Varma, Rev. Mod. Phys. **48**, 219 (1976).
[3]N. Grewe, Solid State Commun. **50**, 19 (1984).
[4]B. H. Brandow, Phys. Rev. B **33**, 215 (1986).
[5]C. Lacroix, J. Magn. Magn. Mater. **63&64**, 239 (1987).
[6]P. Wachter and G. Travaglini, J. Magn. Magn. Mater. **47&48**, 423 (1985).
[7]F. Marabelli and P. Wachter, in *Theoretical and Experimental Aspects of Valence Fluctuations and Heavy Fermions,* edited by L. C. Gupta and S. V. Malik (Plenum, New York, 1987), p. 269.
[8]J. Allen, B. Batlogg, and P. Wachter, Phys. Rev. B **20**, 4807 (1979).
[9]G. Travaglini and P. Wachter, Phys. Rev. B **29**, 893 (1984).
[10]G. Travaglini and P. Wachter, Phys. Rev. B **30**, 5877 (1984).
[11]P. Wachter, in *Narrow Band Phenomena—Influence of Electrons with both Band and Localized Character,* edited by J. C. Fuggle, G. A. Sawatzky, and J. W. Allen (Plenum, New York, 1988), p. 67.
[12]H. Boppart, J. Magn. Magn. Mater. **47&48**, 436 (1985).
[13]P. Wachter, in *Handbook on the Physics and Chemistry of Rare Earths,* edited by K. A. Gschneidner, Jr. and L. Eyring (North-Holland, Amsterdam, 1979), Vol. 2, p. 507.
[14]B. Batlogg, E. Kaldis, A. Schlegel, and P. Wachter, Phys. Rev. B **14**, 5503 (1976).
[15]H. J. F. Jansen, A. J. Freeman, and R. Monnier, Phys. Rev. B **31**, 4092 (1985).
[16]B. Batlogg, Phys. Rev. B **23**, 650 (1981).
[17]E. Kaldis, B. Fritzler, E. Jilek, and A. Wisard, J. Phys. Colloq. **40**, C5-366 (1979).
[18]H. Boppart and P. Wachter, Phys. Rev. Lett. **53**, 1759 (1984).
[19]A. Jayaraman, in Ref. 13, Vol. 2, p. 575.
[20]H. Boppart, Ph.D. thesis, ETH Zürich, 1983.
[21]H. Boppart, W. Rehwald, E. Kaldis, and P. Wachter, in *Valence Instabilities,* edited by P. Wachter and H. Boppart (North-Holland, Amsterdam, 1982), p. 81.
[22]G. Schmiester, G. Kaindl, and P. Wachter, in Ref. 7, p. 663.
[23]G. Schmiester, Ph.D. thesis, Freie Universität Berlin, 1987.
[24]H. Bjerrum Møller, S. M. Shapiro, and R. J. Birgeneau, Phys. Rev. Lett. **39**, 1021 (1977).
[25]B. Batlogg, H. R. Ott, and P. Wachter, Phys. Rev. Lett. **42**, 278 (1979).
[26]P. Fischer, W. Hälg, P. Schobinger-Papamantellos, H. Boppart, E. Kaldis, and P. Wachter, in Ref. 21, p. 551.
[27]H. R. Ott and F. Hulliger, Z. Phys. B **49**, 323 (1983).
[28]Y. Lassailly, C. Vettier, F. Holtzberg, A. Benoit, and J. Flouquet, Solid State Commun. **52**, 717 (1984).
[29]D. Wohlleben, J. G. Huber, and M. B. Maple, in *Magnetism and Magnetic Materials (Chicago, 1971),* proceedings of the 17th Annual Conference on Magnetism and Magnetic Materials, AIP Conf. Proc. No. 5, edited by D. C. Graham and J. J. Rhyne (AIP, New York, 1972), p. 1478.
[30]B. Batlogg, H. Boppart, E. Kaldis, D. B. McWhan, and P. Wachter, in Ref. 21, p. 523.
[31]H. J. F. Jansen, A. J. Freeman, and R. Monnier, Phys. Rev. B **33**, 6785 (1986).
[32]The calibration has been performed at room temperature in a steel piston cylinder device with a Teflon cell and a mixture of *n*-pentane and isoamyl alcohol as pressure-transmitting medium.
[33]V. E. Bean, in *High Pressure Measurements Techniques,* edited by G. N. Peggs (Applied Science, London, 1983).
[34]J. D. Thompson, Rev. Sci. Instrum. **55**, 231 (1984).
[35]P. Schwob, Phys. Kondens. Mater. **10**, 186 (1969).
[36]E. Kneller, *Ferromagnetismus* (Springer, Berlin, 1962).
[37]J. Neuenschwander, Ph.D. thesis, ETH Zürich, 1988.
[38]M. E. Fischer, Philos. Mag. **7 II**, 1731 (1962).
[39]Numerical data have been taken from V. F. Sears, AECL-8490, Chalk River, 1984.
[40]A. Jayaraman, V. Narayanamurti, E. Bucher, and R. G. Maines, Phys. Rev. Lett. **25**, 1430 (1970).
[41]See, e.g., J. Rossat-Mignod, in *Handbook of the Physics and Chemistry of the Actinides,* edited by A. J. Freeman and G. H. Lander (North-Holland, Amsterdam, 1984), Vol. 1.
[42]S. W. Lovesy and D. E. Rimmer, Rep. Prog. Phys. **32**, 333 (1969).
[43]I. Mörke and P. Wachter, Solid State Commun. **48**, 441 (1983).
[44]G. Travaglini, F. Marabelli, R. Monnier, E. Kaldis, and P. Wachter, Phys. Rev. B **34**, 3876 (1986).
[45]R. Monnier, J. Rhyner, T. M. Rice, D. D. Koelling, Phys.

Rev. B **31**, 5554 (1985).
[46]M. Konczykowski, P. Haen, J. C. Portal, and J. P. Sénateur, J. Magn. Magn. Mater. **47&48**, 455 (1985).
[47]P. Haen, F. Holtzberg, F. Lapierre, T. Penney, and R. Tournier, in *Valence Instabilities and Related Narrow-Band Phenomena,* edited by R. D. Parks (Plenum, New York, 1977), p. 495.
[48]B. Batlogg, E. Kaldis, and H. R. Ott, Phys. Lett. **62A**, 270 (1977).
[49]Suggested by C. M. Varma (private communication).
[50]D. L. Dexter and R. S. Knox, *Excitons* (Interscience, New York, 1965).
[51]T. M. Rice, in *Solid State Physics,* edited by F. Seitz, D. Turnbull, and H. Ehrenreich (Academic, New York, 1978), Vol. 32, p. 1.
[52]C. Kittel, *Introduction to Solid State Physics,* 5th ed. (Wiley, New York, 1976).
[53]R. S. Knox, *Theory of Excitons, Solid State Physics,* Suppl. 5 (Academic, New York, 1963), p. 100.
[54]D. Jérome, T. M. Rice, and W. Kohn, Phys. Rev. **158**, 462 (1967).
[55]J. Des Cloizeaux, J. Phys. Chem. Solids **26**, 259 (1965).
[56]A. N. Kozlov and L. A. Maksimov, Zh. Eksp. Teor. Fiz. **48**, 1184 (1965) [Sov. Phys.—JETP **21**, 790 (1965)].
[57]L. V. Keldysh and Yu. V. Kopaev, Fiz. Tverd. Tela (Leningrad) **6**, 2791 (1964) [Sov. Phys.—Solid State **6**, 2219 (1965).
[58]B. I. Halperin and T. M. Rice, Rev. Mod. Phys. **40**, 755 (1968).
[59]R. R. Guseĭnov and L. V. Keldysh, Zh. Eksp. Teor. Fiz. **63**, 2255 (1972) [Sov. Phys.—JETP **36**, 1193 (1973)].
[60]B. A. Volkov and V. V. Tugushev, Dokl. Akad. Nauk.—SSSR **265**, 1374 (1982) [Sov. Phys.—Dokl. **27**, 636 (1982)].
[61]J. K. Kübler, Phys. Rev. **183**, 703 (1969).
[62]L. A. Turkevich and M. H. Cohen, Phys. Rev. Lett. **53**, 2323 (1984).
[63]D. E. Logan, J. Chem. Phys. **86**, 234 (1987).
[64]W. Kohn, in *Many-Body Physics,* edited by C. De Witt and R. Balian (Gordon and Breach, New York, 1968), p. 351.
[65]J. A. Wilson and S. Mahajan, Commun. Phys. **2**, 23 (1977); J. A. Wilson, Solid State Commun. **22**, 551 (1977).
[66]N. G. Stoffel, F. Lévy, C. M. Bertoni, and G. Margaritondo, Solid State Commun. **41**, 53 (1982).
[67]B. Schneider, Master's thesis, ETH Zürich, 1983.
[68]G. Busch and H. Schade, *Vorlesungen über Festkörperphysik* (Birkhäuser, Basel, 1973).
[69]I. S. Gradsteyn and I. M. Ryzhik, *Table of Integrals, Series and Products* (Academic, New York, 1965).
[70]W. Shockley, *Electrons and Holes in Semiconductors* (Van Nostrand, New York, 1950), p. 278.
[71]P. Wachter, Lanthanide Actinide Res. **1**, 265 (1986).
[72]C. M. Varma, Solid State Commun. **30**, 537 (1979).
[73]S. Alexander, J. S. Helman, and I. Balberg, Phys. Rev. B **13**, 304 (1976).
[74]C. Vettier, J. Flouquet, J. M. Mignot, and F. Holtzberg, J. Magn. Magn. Mater. **15-18**, 987 (1980).
[75]H. R. Ott, B. Lüthi, and P. S. Wang, in Ref. 47, p. 289.
[76]H. E. Stanley, *Introduction to Phase Transitions and Critical Phenomena* (Clarendon, Oxford, 1971).
[77]W. Gebhardt and U. Krey, *Kritische Phänomene* (Vieweg, Braunschweig, 1980).
[78]I. Frankowski and P. Wachter, in Ref. 21, p. 309.